

Continuum limit of baryon-baryon scattering with SU(3) flavor symmetry

Jeremy R. Green,^{a,1,*} Andrew D. Hanlon,^{b,c,d} Parikshit M. Junnarkar^e and
Hartmut Wittig^{c,d,f}

^aTheoretical Physics Department, CERN, 1211 Geneva 23, Switzerland

^bPhysics Department, Brookhaven National Laboratory, Upton, New York 11973, USA

^cHelmholtz-Institut Mainz, Johannes Gutenberg-Universität, 55099 Mainz, Germany

^dGSI Helmholtzzentrum für Schwerionenforschung, 64291 Darmstadt, Germany

^eInstitut für Kernphysik, Technische Universität Darmstadt, Schlossgartenstraße 2, 64289 Darmstadt, Germany

^fPRISMA Cluster of Excellence and Institut für Kernphysik, University of Mainz, Becher Weg 45, D-55099 Mainz, Germany

E-mail: green@maths.tcd.ie, ahanlon@bnl.gov,

parikshit@theorie.ikp.physik.tu-darmstadt.de, hartmut.wittig@uni-mainz.de

We report a study of the scattering of two octet baryons using lattice QCD. The baryon-baryon spectrum is computed using distillation on eight lattice ensembles spanning six lattice spacings and multiple volumes, all at the SU(3) flavor symmetric point with $m_\pi = m_K \approx 420$ MeV. Using finite-volume quantization conditions, we determine the scattering phase shift and the presence of bound states. Focusing on the H dibaryon, our results show large discretization effects: in the continuum, the binding energy is $B_H = 4.56 \pm 1.13 \pm 0.63$ MeV, whereas on our coarsest lattice spacing this is larger by a factor of about 7.5. We also present preliminary results for a D -wave phase shift and for the spectrum in the nucleon-nucleon 1S_0 channel.

*The 38th International Symposium on Lattice Field Theory, LATTICE2021 26th-30th July, 2021
Zoom/Gather@Massachusetts Institute of Technology*

¹Present address: School of Mathematics and Hamilton Mathematics Institute, Trinity College,
Dublin 2, Ireland

*Speaker

1. Introduction

It is very computationally challenging to study multibaryon systems using lattice QCD. Because of this, past calculations had to make the assumption that discretization effects are small. In these proceedings, we present calculations done at a single SU(3)-symmetric quark mass point, covering a wide range of lattice spacings and several volumes. This allows us to perform the first systematic study of discretization effects in a multibaryon system.

In Section 2, we briefly describe our calculation and in Section 3, we summarize a study of the H dibaryon that was already reported in Ref. [1]. The talk at Lattice 2021 was based on the first version of [1]. Since then, we have revised the analysis by including an additional ensemble and choosing fit regions for determining the spectrum in a more conservative way. These proceedings are based on the revised analysis. For a more complete discussion of the setup of the calculation and the H dibaryon study, we refer the reader to Ref. [1].

The following two sections describe preliminary analyses that extend our work to additional systems: the 1D_2 partial wave (Section 4) and the SU(3) 27-plet (Section 5). Finally, our conclusions are in Section 6.

2. Lattice setup

This calculation is based on eight ensembles generated by CLS [2], with three degenerate quarks that have a mass set to the average of the physical u , d , and s quark masses, corresponding to $m_\pi = m_K \approx 420$ MeV. The ensembles span six lattice spacings and a range of volumes, as shown in Fig. 1.

Our analysis is based on finite-volume spectroscopy and quantization conditions. In a given symmetry sector, we compute a matrix of two-point correlation functions,

$$C_{ij}(t) \equiv \langle \mathcal{O}_i(t) \mathcal{O}_j^\dagger(0) \rangle, \quad (1)$$

where the two-baryon interpolating operators $\{\mathcal{O}_j\}$ are formed from linear combinations of products of momentum-projected single-baryon interpolators. In addition to definite flavor, total momentum \vec{P} , and irreducible representation of the little group of \vec{P} , the operators also have a definite two-baryon spin.

To determine the spectrum, we solve a generalized eigenvalue problem, $C(t_D)v_n = \lambda_n C(t_0)v_n$, and use the eigenvectors to construct an approximately diagonalized correlator matrix $\tilde{C}(t)$ with diagonal entries approximately proportional to $e^{-E_n t}$ at large t . We form the ratio of $\tilde{C}_n(t)$ to a product of two single-baryon correlators and perform fits to obtain the shift ΔE_n from the corresponding noninteracting level.

Finite-volume quantization conditions [3–6] provide a relation between the spectrum and the baryon-baryon scattering amplitude. We use a form similar to Ref. [7], which says that the spectrum

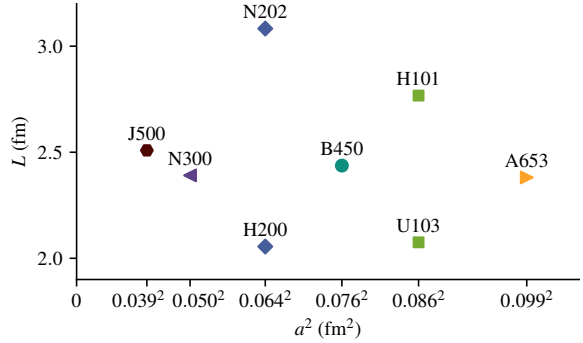


Figure 1: Box size L and lattice spacing a for the ensembles used in this work.

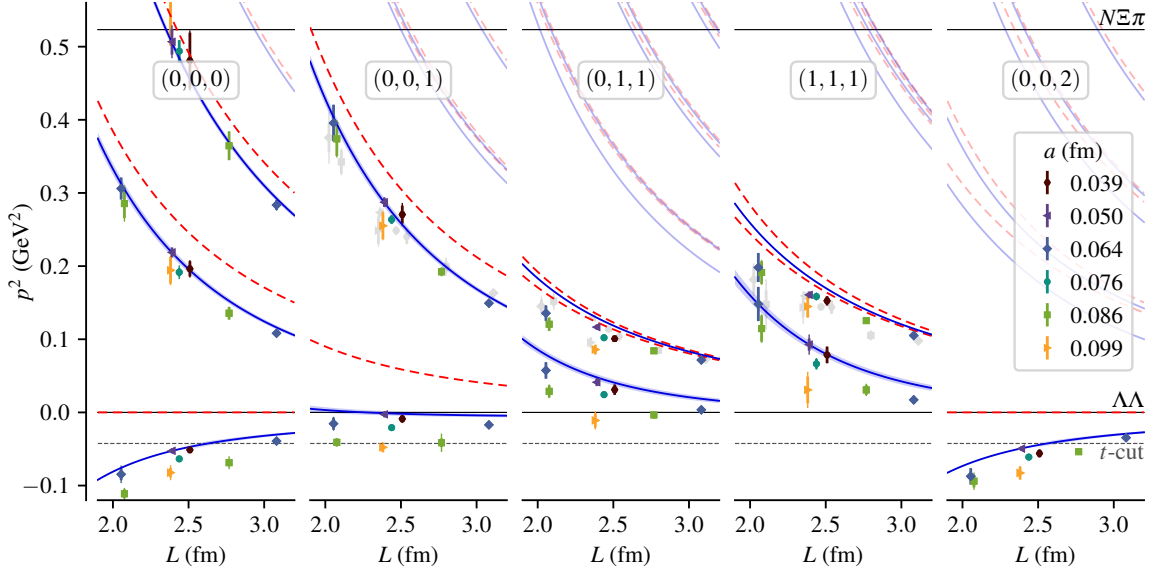


Figure 2: Singlet spectrum in trivial irreps: p^2 versus L in the rest frame and four moving frames. The colored and gray points show lattice spin-zero and spin-one energy levels, respectively. The blue curves show the energy levels in the continuum obtained from a global fit and the red dashed curves show the noninteracting levels.

is given by solutions of

$$\det [\tilde{K}^{-1}(p^2) - B(p^2)] = 0, \quad (2)$$

where \tilde{K} contains the scattering amplitude and B depends on the volume, \vec{P} , and irrep. In this work, our preferred kinematic variable is the center-of-mass momentum $p^2 \equiv (E_{\text{cm}}/2)^2 - m_B^2$.

We study the scattering of two octet baryons. The flavor content of this baryon-baryon system belongs to one of five $SU(3)$ irreps:

$$\mathbf{8} \otimes \mathbf{8} = (\mathbf{1} \oplus \mathbf{8} \oplus \mathbf{27})_S \oplus (\mathbf{8} \oplus \mathbf{10} \oplus \overline{\mathbf{10}})_A, \quad (3)$$

where the subscripts denote irreps appearing in the symmetric and antisymmetric products. The simplest irreps to study are the singlet and septenvigintuplet, since they appear only in the symmetric product, meaning that even partial waves have spin zero and do not couple to other partial waves. In particular, our initial focus is on the H dibaryon, which appears in the singlet 1S_0 channel.

3. H dibaryon (singlet S -wave)

The H dibaryon is a conjectured $uudds$ bound state that is a scalar and an $SU(3)$ singlet [8]. Lattice calculations performed with dynamical fermions agree that this bound state exists for heavier-than-physical quark masses but do not agree on its binding energy, with results varying from a few MeV up to 75 MeV.

The $SU(3)$ singlet baryon-baryon spectra from our calculation, in the trivial irrep of the rest frame and in four moving frames and on all ensembles, are shown in Fig. 2. One can see a clear trend as the lattice spacing is varied, with coarser lattice spacings corresponding to lower energies that are further below the noninteracting levels.

Given the energy levels at nonzero lattice spacing, our goal is to obtain the continuum phase shift. Two strategies for this are illustrated in Fig. 3. Conceptually, it is most straightforward to follow the red path, by performing continuum extrapolations of the finite-volume energy levels and then obtain the scattering amplitude using quantization conditions, which have been derived in the continuum. However, in practice this is difficult because it requires matched volumes at multiple lattice spacings. Alternatively, one can follow the blue path by first obtaining a scattering amplitude at finite lattice spacing and then extrapolating it to the continuum. However, this requires a quantization condition at finite lattice spacing, which has only been studied for a simple model in Ref. [9].

Our strategy is to defer a rigorous understanding of quantization conditions and scattering amplitudes at finite lattice spacing to future work. Instead, we apply continuum quantization conditions to data at nonzero lattice spacing and assume that symmetry-breaking effects are small so that the effect of lattice artifacts is to only modify the parameters of a continuum scattering amplitude.

Truncated to S -wave, the quantization condition becomes

$$p \cot \delta_0(p^2) = B_{00}(p^2) \equiv \frac{2}{\sqrt{\pi} L \gamma} Z_{00}^{\vec{P}L/(2\pi)} \left(1, \left(\frac{pL}{2\pi} \right)^2 \right), \quad (4)$$

where $Z_{00}^{\vec{D}}$ is a generalized zeta function. Given an energy level corresponding to momentum p^2 , this provides the phase shift $\delta_0(p^2)$ at that scattering momentum. Conversely, given an ansatz for $\delta_0(p^2)$, the solutions to this equation provide the finite volume spectrum.

We determine $\delta_0(p^2)$ in the continuum by performing global fits to the spectra from all of our ensembles. Our fit ansatz assumes that $p \cot \delta_0(p^2)$ can be described by a polynomial in p^2 ,

$$p \cot \delta_0(p^2) = \sum_{i=0}^{N-1} c_i p^{2i}, \quad c_i = c_{i0} + c_{i1} a^2. \quad (5)$$

We use the quantization condition to transform this ansatz for $\delta_0(p^2)$ into an ansatz for the spectrum, and fit to the spectrum. States below the t -channel cut or above the inelastic cut are excluded from our fits. In addition, we exclude the excited states in frames $(0, 1, 1)$ and $(1, 1, 1)$ because a nonzero D -wave amplitude is needed to describe them (see the next section).

Bound states correspond to poles on the physical sheet of the scattering amplitude below threshold, i.e. for $p = i\kappa$, $\kappa > 0$. They can be found by solving for $p \cot \delta(p) = -\sqrt{-p^2}$. In all cases, we find a bound H dibaryon. The binding energy depends strongly on the lattice spacing, as shown in Fig. 4. Our final result is $B_H = 4.56 \pm 1.13 \pm 0.63$ MeV, where the second (systematic) uncertainty is obtained by varying the plateau region used to obtain the spectra and by performing

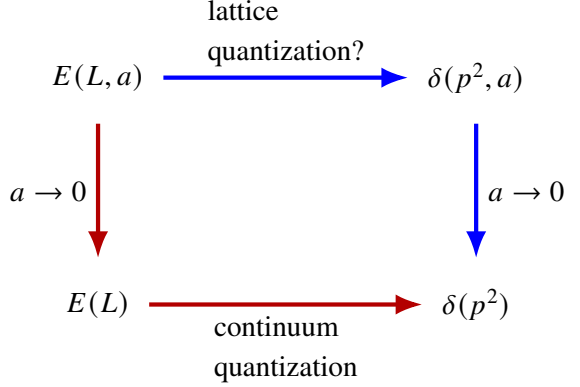


Figure 3: Two paths, red and blue, from the lattice finite-volume energy levels $E(L, a)$ to the continuum phase shift $\delta(p^2)$.

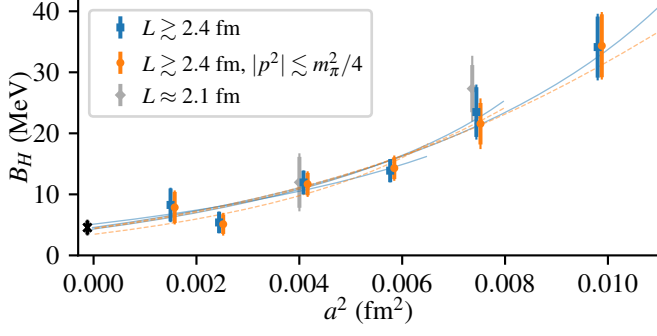


Figure 4: Binding energy of the H dibaryon versus squared lattice spacing. The points are obtained from analyzing individual ensembles and the curves are from global fits to the spectra on multiple ensembles.

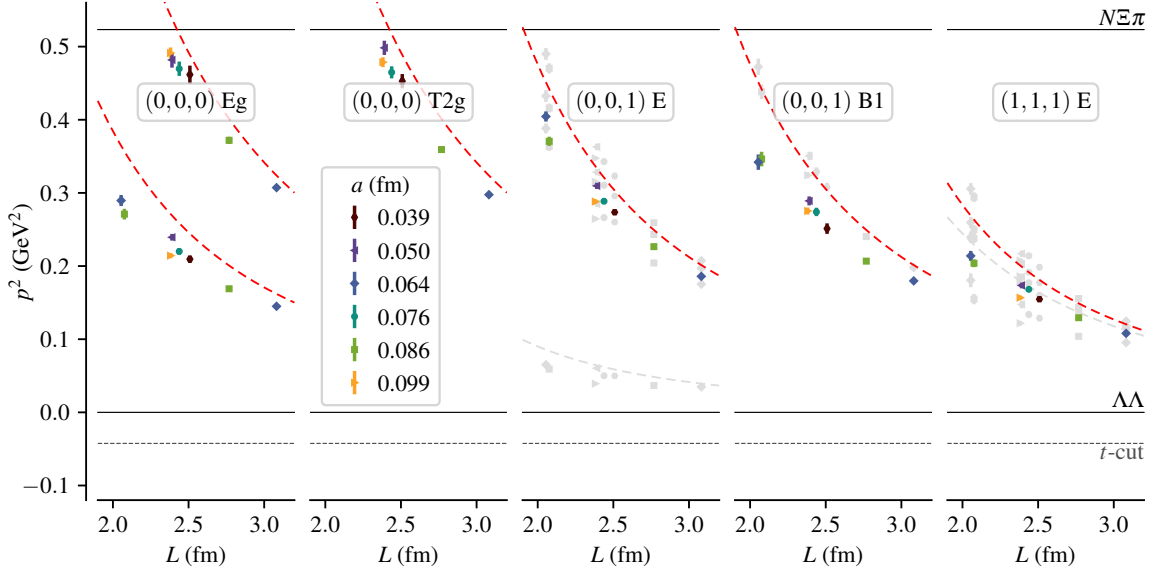


Figure 5: Singlet spectrum in nontrivial irreps containing spin-zero states. Spin-one states and spin-one noninteracting levels are shown in grey; see the caption of Fig. 2.

cuts on a , L , and p^2 . For further details about the analysis, including a cross-check based on the red path in Fig. 3, see Ref. [1].

4. Singlet D -wave (preliminary)

Nontrivial irreps provide information about higher partial waves. Figure 5 shows preliminary estimates of $SU(3)$ singlet energy levels relevant for the 1D_2 partial wave. Here we rely on overlaps between states and interpolating operators to identify the spin-zero states; in some cases, there are many more spin-one states.

For this flavor channel, both \tilde{K} and B are diagonal in spin, so that the quantization condition factorizes and spin zero can be analyzed independently of spin one. Neglecting G -wave and higher partial waves, the quantization condition for the irreps in Fig. 5 has the form

$$\det [p^5 \cot \delta_2(p^2) I_{n \times n} - B(p^2)] = 0, \quad (6)$$

where I is the $n \times n$ identity matrix, $B(p^2)$ is a matrix involving generalized zeta functions, and

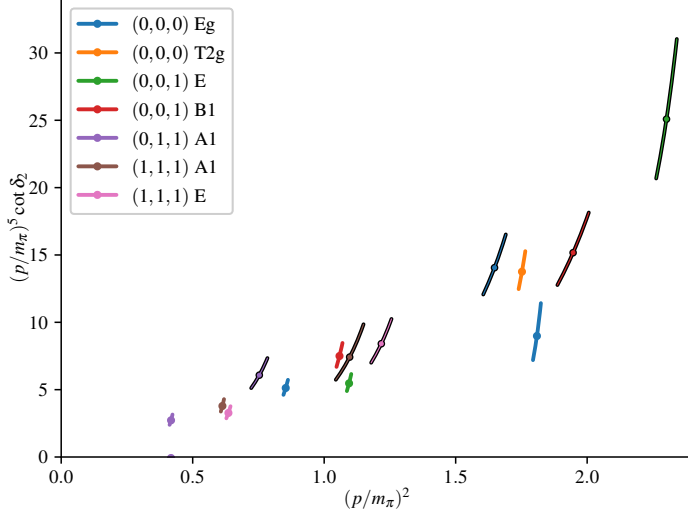


Figure 6: Singlet $p^5 \cot \delta_2(p^2)$ versus p^2 , in units of the pion mass, for ensembles N202 (solid colors) and H200 (with black outlines). For irreps with two solutions, just one of them appears within the bounds of this plot.

$n = 1$ or 2 . Given an energy level corresponding to momentum p^2 , the eigenvalues of $B(p^2)$ provide the one or two possible values of $p^5 \cot \delta_2(p^2)$.

We also return to the trivial A1 irrep in frames $(0, 1, 1)$ and $(1, 1, 1)$, for which we were unable to describe the excited-state energy using only S wave. Including both S and D waves, we get

$$\det \left[\begin{pmatrix} p \cot \delta_0(p^2) & 0_{1 \times n} \\ 0_{n \times 1} & p^5 \cot \delta_2(p^2) I_{n \times n} \end{pmatrix} - \begin{pmatrix} B_{00}(p^2) & B_{02}(p^2) \\ B_{20}(p^2) & B_{22}(p^2) \end{pmatrix} \right] = 0. \quad (7)$$

Taking the Schur complement, we obtain

$$p \cot \delta_0(p^2) = B_{00}(p^2) + B_{02}(p^2) [p^5 \cot \delta_2(p^2) I_{n \times n} - B_{22}(p^2)]^{-1} B_{20}(p^2). \quad (8)$$

The fact that the low-lying spin-zero noninteracting levels are singly degenerate implies that the matrix $B(p^2)$ has just one divergent eigenvalue at each of these levels. From this, we find that the RHS of Eq. (8) has a pole only when $\det[p^5 \cot \delta_2(p^2) I_{n \times n} - B_{22}(p^2)] = 0$. If $\delta_2(p^2) = 0$, this reduces to the noninteracting levels. In general, if $\delta_0(p^2)$ does not pass through zero, then an interacting level will be found between every pair of poles. As seen in Fig. 2, describing our data requires that the poles be shifted from the noninteracting levels, which implies a nonzero $\delta_2(p^2)$.

Taking the Schur complement in the opposite way, we find that the possible values of $p^5 \cot \delta_2(p^2)$ are given by eigenvalues of

$$B_{22}(p^2) + \frac{B_{20}(p^2)B_{02}(p^2)}{p \cot \delta_0(p^2) - B_{00}(p^2)}. \quad (9)$$

As a first study, we fix $\delta_0(p^2)$ based on fits to other levels in trivial irreps. With this fixed, we find that the excited state in frames $(0, 1, 1)$ and $(1, 1, 1)$ provides a good constraint on $\delta_2(p^2)$. Preliminary results are shown in Fig. 6 for two ensembles, N202 and H200, with the same lattice spacing but different volumes. The D -wave phase shift obtained from these levels is quite compatible with the phase shift obtained from nontrivial irreps where S -wave does not contribute. Furthermore, these levels are particularly useful because they have the smallest p^2 and provide information closest to the threshold. We also note that a nonrelativistic version of the analysis in Ref. [10] could help to explain why these levels are primarily influenced by D wave.

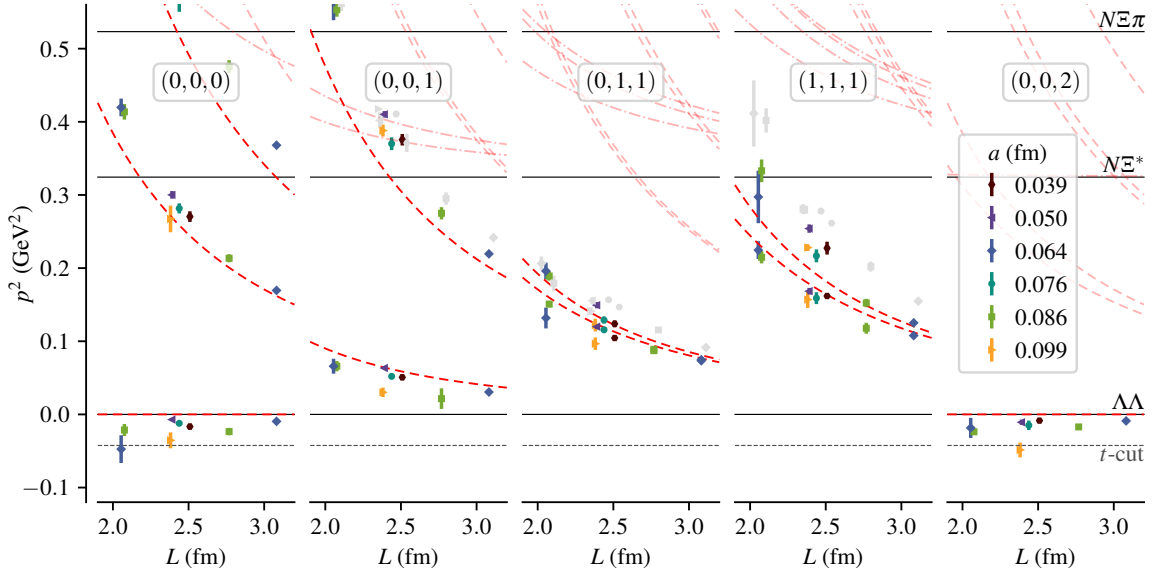


Figure 7: Septenvigtuplet spectrum in trivial irreps. In addition to the dashed curves showing noninteracting octet-octet levels, we also show dash-dotted curves depicting noninteracting octet-decuplet levels.

5. 27-plet S -wave (preliminary)

The other $SU(3)$ flavor irrep that appears only in the symmetric product of two octet baryons is the 27-plet. This is particularly interesting because it contains the nucleon-nucleon isospin-one channel, where some calculations using a single lattice spacing have reported a bound “dineutron” state [11–14]. Here the inelastic threshold is lower, corresponding to $m_B + m_D$, where m_B and m_D are the octet and decuplet baryon masses. Although the octet-decuplet channel could be included in two-particle quantization conditions, we do not include the relevant octet-decuplet interpolating operators; therefore, our usable range of spectrum is smaller in the 27-plet.

Preliminary estimates of the spectra in trivial irreps are shown in Fig. 7. Near threshold, the downward shifts from noninteracting levels are considerably smaller than in the singlet sector, rendering a bound state rather unlikely. Higher in the spectrum, the levels are shifted upward from the noninteracting ones; this indicates that at some point the phase shift passes through zero. Because of this, $p \cot \delta_0(p^2)$ cannot be well described by polynomials, and we are exploring other fit forms such as rational functions. The absolute size of the discretization effects is perhaps a bit smaller than in the singlet sector; however, since the shifts from noninteracting levels are also smaller, the relative effect on the phase shift may still be large.

6. Conclusions

Using distillation, we are able to determine the low-lying spectrum of baryon-baryon states in a variety of frames, irreps, and flavor channels, which can then be analyzed using finite-volume quantization conditions. We have repeated this using several lattice ensembles with six different lattice spacings, producing the first study of discretization effects in a multibaryon system. Our results show a strong dependence on the lattice spacing, which makes it essential to include a

continuum limit study: the binding energy of the H dibaryon on our coarsest lattice spacing is about 7.5 times larger than in the continuum.

This work is currently being extended in two ways. First, we are studying other systems at the $SU(3)$ -symmetric point, in particular nucleon-nucleon scattering. Second, we are studying the effect of $SU(3)$ breaking and the approach to the physical point [15].

Acknowledgments

We thank Dorota M. Grabowska, Maxwell T. Hansen, Ben Hörz, and Daniel Mohler for helpful conversations. Calculations for this project used resources on the supercomputers JUQUEEN [16], JU-RECA [17], and JUWELS [18] at Jülich Supercomputing Centre (JSC). The authors gratefully acknowledge the support of the John von Neumann Institute for Computing and Gauss Centre for Supercomputing e.V. (<http://www.gauss-centre.eu>) for project HMZ21. The raw distillation data were computed using QDP++ [19], PRIMME [20], and the deflated SAP+GCR solver from openQCD [21]. Contractions were performed with a high-performance BLAS library using the Python package `opt_einsum` [22]. The correlator analysis was done using SigMonD [23]. Much of the data handling and the subsequent phase shift analysis was done using NumPy [24] and SciPy [25]. The plots were prepared using Matplotlib [26]. The quantization condition beyond S -wave was computed using TwoHadronsInBox [7]. This research was partly supported by Deutsche Forschungsgemeinschaft (DFG, German Research Foundation) through the Cluster of Excellence “Precision Physics, Fundamental Interactions and Structure of Matter” (PRISMA+ EXC 2118/1) funded by the DFG within the German Excellence Strategy (Project ID 39083149), as well as the Collaborative Research Centers SFB 1044 “The low-energy frontier of the Standard Model” and CRC-TR 211 “Strong-interaction matter under extreme conditions” (Project ID 315477589 – TRR 211). ADH is supported by: (i) The U.S. Department of Energy, Office of Science, Office of Nuclear Physics through the Contract No. DE-SC0012704 (S.M.); (ii) The U.S. Department of Energy, Office of Science, Office of Nuclear Physics and Office of Advanced Scientific Computing Research, within the framework of Scientific Discovery through Advance Computing (SciDAC) award Computing the Properties of Matter with Leadership Computing Resources. JRG acknowledges support from the Simons Foundation through the Simons Bridge for Postdoctoral Fellowships scheme. We are grateful to our colleagues within the CLS initiative for sharing ensembles.

References

- [1] J.R. Green, A.D. Hanlon, P.M. Junnarkar and H. Wittig, *Weakly bound H dibaryon from $SU(3)$ -flavor-symmetric QCD*, *Phys. Rev. Lett.* (to be published) (2021) [2103.01054].
- [2] M. Bruno et al., *Simulation of QCD with $N_f = 2 + 1$ flavors of non-perturbatively improved Wilson fermions*, *JHEP* **02** (2015) 043 [1411.3982].
- [3] M. Lüscher, *Two-particle states on a torus and their relation to the scattering matrix*, *Nucl. Phys. B* **354** (1991) 531.
- [4] K. Rummukainen and S.A. Gottlieb, *Resonance scattering phase shifts on a non-rest-frame lattice*, *Nucl. Phys. B* **450** (1995) 397 [hep-lat/9503028].
- [5] R.A. Briceño, Z. Davoudi and T.C. Luu, *Two-nucleon systems in a finite volume: Quantization conditions*, *Phys. Rev. D* **88** (2013) 034502 [1305.4903].
- [6] R.A. Briceño, *Two-particle multichannel systems in a finite volume with arbitrary spin*, *Phys. Rev. D* **89** (2014) 074507 [1401.3312].

- [7] C. Morningstar, J. Bulava, B. Singha, R. Brett, J. Fallica, A. Hanlon et al., *Estimating the two-particle K -matrix for multiple partial waves and decay channels from finite-volume energies*, *Nucl. Phys. B* **924** (2017) 477 [1707.05817].
- [8] R.L. Jaffe, *Perhaps a stable dihyperon*, *Phys. Rev. Lett.* **38** (1977) 195.
- [9] C. Körber, E. Berkowitz and T. Luu, *Renormalization of a contact interaction on a lattice*, 1912.04425.
- [10] D.M. Grabowska and M.T. Hansen, *Analytic expansions of multi-hadron finite-volume energies: I. Two-particle states*, 2110.06878.
- [11] T. Yamazaki, K.-i. Ishikawa, Y. Kuramashi and A. Ukawa, *Study of quark mass dependence of binding energy for light nuclei in $2 + 1$ flavor lattice QCD*, *Phys. Rev. D* **92** (2015) 014501 [1502.04182].
- [12] E. Berkowitz, T. Kurth, A. Nicholson, B. Joó, E. Rinaldi, M. Strother et al., *Two-nucleon higher partial-wave scattering from lattice QCD*, *Phys. Lett. B* **765** (2017) 285 [1508.00886].
- [13] NPLQCD collaboration, *Baryon-baryon interactions and spin-flavor symmetry from lattice quantum chromodynamics*, *Phys. Rev. D* **96** (2017) 114510 [1706.06550].
- [14] NPLQCD collaboration, *Low-energy scattering and effective interactions of two baryons at $m_\pi \sim 450$ MeV from lattice quantum chromodynamics*, *Phys. Rev. D* **103** (2021) 054508 [2009.12357].
- [15] M. Padmanath et al., *H dibaryon away from the $SU(3)_f$ symmetric point*, *PoS LATTICE2021* 459.
- [16] Jülich Supercomputing Centre, *JUQUEEN: IBM Blue Gene/Q supercomputer system at the Jülich Supercomputing Centre*, *J. Large-Scale Res. Facil.* **1** (2015) A1.
- [17] Jülich Supercomputing Centre, *JURECA: Modular supercomputer at Jülich Supercomputing Centre*, *J. Large-Scale Res. Facil.* **4** (2018) A132.
- [18] Jülich Supercomputing Centre, *JUWELS: Modular tier-0/1 supercomputer at the Jülich Supercomputing Centre*, *J. Large-Scale Res. Facil.* **5** (2019) A135.
- [19] SciDAC, LHPC, UKQCD collaboration, *The Chroma software system for lattice QCD*, *Nucl. Phys. B (Proc. Suppl.)* **140** (2005) 832 [hep-lat/0409003].
- [20] A. Stathopoulos and J.R. McCombs, *PRIMME: PReconditioned Iterative MultiMethod Eigensolver—methods and software description*, *ACM Trans. Math. Softw.* **37** (2010) 21:1.
- [21] M. Lüscher and S. Schaefer, “openQCD.” <http://luscher.web.cern.ch/luscher/openQCD/>, 2012.
- [22] D.G.A. Smith and J. Gray, *opt_einsum - A Python package for optimizing contraction order for einsum-like expressions*, *J. Open Source Softw.* **3(26)** (2018) 753.
- [23] C. Morningstar, “SigMonD.” <https://github.com/andrewhanlon/sigmond>, Feb., 2021.
- [24] C.R. Harris, K.J. Millman, S.J. van der Walt, R. Gommers, P. Virtanen, D. Cournapeau et al., *Array programming with NumPy*, *Nature* **585** (2020) 357 [2006.10256].
- [25] P. Virtanen, R. Gommers, T.E. Oliphant, M. Haberland, T. Reddy, D. Cournapeau et al., *SciPy 1.0: fundamental algorithms for scientific computing in Python*, *Nature Methods* **17** (2020) 261 [1907.10121].
- [26] J.D. Hunter, *Matplotlib: A 2D graphics environment*, *Comput. Sci. Eng.* **9** (2007) 90.